Diffusion of Zn in AZ91 and in QE22 reinforced by Saffil fibers

J. Čermák, I. Stloukal

Diffusion of ^{65}Zn in AZ91 and in QE22 reinforced by Saffil fibers

J. Čermák, I. Stloukal

PII: S0266-3538(07)00267-9
DOI: 10.1016/j.compscitech.2007.06.017
Reference: CSTE 3758

To appear in: *Composites Science and Technology*

Received Date: 10 April 2007
Revised Date: 19 June 2007
Accepted Date: 21 June 2007

Please cite this article as: Čermák, J., Stloukal, I., Diffusion of ^{65}Zn in AZ91 and in QE22 reinforced by Saffil fibers, *Composites Science and Technology* (2007), doi: 10.1016/j.compscitech.2007.06.017

Diffusion of ^{65}Zn in AZ91 and in QE22 reinforced by Saffil fibers

J. Čermák, I. Stloukal

Institute of Physics of Materials AS CR, v. v. i., Žižkova 22, CZ-616 62, Czech Republic

Abstract

Effective diffusion coefficients D_{eff} of radioisotope ^{65}Zn in Mg-based alloys AZ91 and QE22 with short Saffil fibers were measured by serial sectioning method in the temperature interval 648 – 728 K. The results were compared with ^{65}Zn volume diffusion coefficients D_v obtained with the same materials without the reinforcement. This enabled to assess the influence of the interfaces between the matrix and the fibers upon the effective diffusion coefficients and to estimate the diffusion coefficients D_i of Zn in Saffil/matrix interphase boundaries. It was observed that temperature dependence of both D_{eff} and D_i is significantly concave in the studied temperature interval, which was ascribed to relaxation of thermo-elastic stresses present in the composite as a consequence of considerable differences between the coefficients of thermal expansion (CTE) of both the constituents. D_{eff} and D_i tend to higher values close to 693 K, where the CTE is in a local minimum – i.e., where the maximum dislocation density by the phase interface can be expected.

Keywords: A. Metal-matrix composites (MMCs); A. Short-fiber composites; B. Interface; B. High-temperature properties; Diffusion

1. Introduction

There is a number of commercial Mg-based alloys that are designed before all as structural materials for aircraft and automotive industry. As for the alloying elements added to pure Mg, four elements are most frequently applied: Mn, Al, Zn, Zr and a mixture of rare earths (RE) metals. They are grouped into following combinations Mg + (Mn), Mg + (Al, Mn), Mg + (Al, Zn, Mn), Mg + (Zr), Mg + (Zn, Zr), Mg + (RE, Zr), Mg + (Ag, RE, Zr) or Mg + (Y, RE, Zr) making the various alloy families. In order to enhance mechanical strength, some of the grades are reinforced by particles or fibers made from carbon, SiO_2, Al_2O_3 and other materials.

An example of the "general-purpose" alloys that are frequently used is AZ91 and some applications found also QE22 [1]. These alloys represent two of the above mentioned alloy families.

Studies revealing the mechanical parameters of AZ91 and QE22 are reviewed, e.g., in [1], the influence of fibers and, especially, the role of interface between the matrix and the fibers are reported for example in [2-6].

Since the alloys are subjected to temperature treatment during the production process and to thermal cycling in the course of the service, it is clear that the knowledge of diffusion characteristics is highly important for the estimation of the rate of all diffusion-controlled processes in the material. The reinforced versions of the both alloys contain internal interfaces between the fibers and the matrix that may act as short-circuit paths of diffusion. They may play a significant role in the kinetics of diffusion-controlled processes running in the composites. Moreover, the dramatic difference in the coefficient of thermal expansion (CTE) of fibers and matrix causes thermo-elastic

stresses that should be considered as another significant factor influencing the atomic mobility in the area close to the interface.

In the present paper, diffusion of ^{65}Zn in Mg-based alloys AZ91S and QE22S with short Saffil fibers was studied by serial sectioning method in the temperature interval 648 - 728 K, where the temperature dependence of CTE shows a local minimum [5]. The obtained effective diffusion coefficients of the two-phase alloys were compared with coefficients of bulk diffusion obtained in the measurements made with the same materials without the reinforcement, which enabled to estimate interface diffusion coefficients of ^{65}Zn in interphase boundaries between the fibers and matrix.

2. Experimental details

2.1.Experimental alloys

Experimental alloys AZ91S and QE22S (ASTM notation [1]; S stands for Saffil reinforcement) were produced by squeeze casting at the Technical University Clausthal-Zellerfeld, Germany. Nominal composition of AZ91S and QE22S was Mg – 8.7 wt. % Al – 1 % wt. Zn – 0.13 wt. % Mn, and Mg – 2.5 wt. % Ag – 2.1 wt. % Di – 0.7 wt. % Zr respectively (Di – *didymium* is a mixture of rare earth elements made up chiefly of Nd and Pr). The volume fraction of the Saffil (97 % δ-Al_2O_3 + 3 % SiO_2) fibers in AZ91S and QE22S was 25 and 44 vol. % respectively, which was checked by digital image analysis of SEM micrographs. The mean length of Saffil fibers was about 50 μm and diameter some 4 μm.

The measurement of ^{65}Zn diffusion coefficients was carried out also with samples without the Saffil reinforcement (AZ91 and QE22). They were machined from the same ingots using their marginal part without the Saffil sponge.

The structure of AZ91 is composed typically of primary solid solution (Mg) and $Mg_{17}Al_{12}$ precipitates present as massive precipitates and as a component of very fine eutectic. Strengthened version of the alloy contains ceramic Saffil fibers that do not react considerably with the matrix [7]. The QE22 consists of grains of (Mg) solid solution decorated by $Mg_{9-12}Di$ phase.

2.2. Diffusion samples and the thermal pre-treatment

Cylinder diffusion samples with diameter 10 mm and height 4 mm were machined from the ingots in a way that prevailing direction of fibers was parallel to the diffusion direction (parallel to the axis of cylindrical samples).

The goal of the present study was to reveal the influence of the fiber/matrix interface upon the diffusion characteristics of the composite. Therefore, the presence of any other interfaces that may act as short-circuit paths for diffusion and that may mask the diffusion along the fiber/matrix interfaces was undesirable. This was the reason for the pre-annealing of samples made from AZ91 and AZ91S alloys at 693 K for 15 h in pure (6N) Ar. It was aimed to dissolve the eutectic with high density of (Mg)/$Mg_{17}Al_{12}$ inter-phase boundaries. Similar thermal treatment – anneal at 798 K / 8 h / Ar – was applied also to the samples made from alloys QE22 and QE22S.

The structure of pre-annealed samples was stabilized by additional annealing at respective diffusion temperature T for the time t, which simulated the diffusion anneals (see in Tables 1, 2). Diffusion temperatures for both alloys were chosen in the area of primary solid solution (Mg) in AZ91 [8,9]. The final structure is illustrated in Figs. 1-5. The structure of treated samples of AZ91 alloy consists of relatively large grains (mean intercept d ~ 150 μm) – see Fig. 1. Grain boundaries were anchored by thin $Mg_{17}Al_{12}$

precipitates as can be seen in the polarized light. In AZ91S, fine particles of $Mg_{17}Al_{12}$ precipitated preferentially at the surface of Saffil fibers (see light particles in Fig. 2).

The mean grain size of QE22 alloy after the treatment was about the same as that in AZ91 alloy (Fig. 3). As a second phase, Nd-rich precipitates were detected that were located often at grain boundaries. They resulted from partial solution and coalescence of the magnesium-*didymium* eutectic [1,10]. Neither silver nor aluminum was detected in the particles by SEM, therefore the presence of ternary precipitates $(Mg, Ag)_{12}Nd$, $Mg_{12}Nd_2Ag$ observed in [11] and Al-containing precipitates $(Al_xMg_{1-x})Nd$ [10] can be excluded. The same particles are present also in QE22S (Fig. 4) where they are located preferentially at the surface of fibers, which is illustrated in detailed micrograph in Fig. 5. The direction of diffusion flux was in the plane of fibers in the pre-forma (Figs. 2, 4). The orientation of samples was found by trial prism cut from the received block of material.

2.3. Diffusion measurement

The samples were mechanically polished using standard metallographic methods. The radioisotope ^{65}Zn was deposited by vacuum evaporation technique using the 0.1M water solution of $^{65}ZnCl_2$ with the specific activity 9.24 MBq mg^{-1} Zn. The carrier was dripped-and-dried onto tungsten boat, thermally decomposed in vacuum (~ 3×10^{-6} mbar) and evaporated on cold samples. After the deposition of thin radioactive layer, the samples were wrapped in protective Ta thin foil, sealed in silica ampoules with pure Ar and annealed in horizontal furnace at temperatures stabilized within ± 1 K. Measurement of penetration profiles – $c(x,t)$ (c, x, t – concentration of ^{65}Zn, depth co-ordinate and diffusion time, respectively) followed by the serial sectioning technique

using the microtome Leica RM2255 for sectioning the diffusion zone. Concentration measurement was made with the help of Liquid Scintillation Counter TRI-CARB 3170 TR/LS.

3. Results and discussion

3.1. Penetration profiles

Measured penetration profiles $c(x,t)$ are shown in Figs. 6-9. It is obvious that they are linear in co-ordinates log c vs x^2 over several orders of magnitude in all the cases. This is evidence that the diffusion can be described by volume diffusion coefficient in alloys without fibers and by effective diffusion coefficient in reinforced alloys. No potential high-diffusivity paths present in the samples (such as grain boundaries and interphase planes) affected individually the measured profiles in a sense of known diffusion kinetics described, e.g., in [12]. Hence, the diffusion coefficients D were obtained by fitting known *thin-film-solution* [13]

$$c(x,t) = \frac{M}{\sqrt{\pi D t}} \exp\left(-\frac{x^2}{4 D t}\right), \quad (1)$$

where M stands for the surface concentration at $t = 0$ and D is either volume diffusion coefficient (D_v) for alloys without or effective diffusion coefficient (D_{eff}) for alloys with Saffil fibers. Eq. (1) was fitted to penetration profiles and unknown constants M and D were found as fit parameters. Results of the optimization procedure are summarized in Tables 1, 2. Typical errors were about 5 % by D_v and 20 % by D_{eff}.

Comparing the values of mean diffusion path L listed in Tables 1, 2 with the structures in Figs. 2, 4, it can be concluded that L's are greater than the typical distance between the fibers and, at the same time, much greater than typical diameter of fibers.

This implies that the diffusion in reinforced alloys can be well described by an effective diffusion coefficient D_{eff} [12].

3.2. Effective diffusivity

It can be seen in Tables 1, 2 that values of D_{eff} are always higher than those of D_{v}. Bearing in mind that it can be expected that the volume diffusion in alumina in general is much slower [14] than that in AZ91 and QE22, it can be concluded that the difference between D_{eff} and D_{v} should be due to the fast diffusion along interface Saffil/matrix. In [15], relation

$$D_{\mathrm{eff}} = \frac{D_{\mathrm{i}}}{\left(g_{\mathrm{i}} + \frac{g_1}{s_1} + \frac{g_2}{s_2} \right)} \frac{1 - 2\, g_1 \frac{D_{\mathrm{i}}\, s_1 - D_1}{2\, D_{\mathrm{i}}\, s_1 + D_1} - 2\ \ g_2 \frac{D_{\mathrm{i}}\, s_2 - D_2}{2\, D_{\mathrm{i}}\, s_2 + D_2}}{1 + g_1 \frac{D_{\mathrm{i}}\, s_1 - D_1}{2\, D_{\mathrm{i}}\, s_1 + D_1} + g_2 \frac{D_{\mathrm{i}}\, s_2 - D_2}{2\, D_{\mathrm{i}}\, s_2 + D_2}} \tag{2}$$

between the effective diffusivity D_{eff} and diffusivities in the two phases (indices 1 and 2) separated by interphase boundary of diffusivity D_{i} (g and s are volume fractions and segregation factors of respective phases) was proposed. If we presume in the present case that the diffusion of ^{65}Zn in interfaces is much faster than that in alumina and in the matrix ($D_{\mathrm{i}} >> D_1, D_2$) and that zinc does not segregate considerably to the near-interface area both in the matrix and in the fiber ($s_1, s_2 \sim 1$), we obtain, after elementary re-arrangements, for the interface diffusivity

$$D_{\mathrm{i}} = \frac{2 + g_1 + g_2}{2\, g_{\mathrm{i}}}\, D_{\mathrm{eff}}\,. \tag{3}$$

Considering cylinder shape of fibers with typical diameter ~ 4 μm, length 50 μm and thickness of interface $\delta \sim 5 \times 10^{-10}$ m (commonly accepted grain boundary thickness

[12]), we can estimate volume fraction of fibers g_1 ~ 0.25 in AZ91S, g_1 ~ 0.44 in QE22S. Finally, we obtain approximate relation

$$D_i \cong 1.20 \times 10^4 \; D_{eff} \quad (4)$$

for D_i in AZ91S and

$$D_i \cong 6.89 \times 10^3 \; D_{eff} \quad (5)$$

for D_i in QE22S. Calculated values of D_i for both alloys are summarized in Tables 1, 2. Their typical error is the same as error of D_{eff} (~ 20 %).

3.3. Temperature dependence of D_v

Temperature dependence of obtained values of volume diffusion coefficients D_v is shown in Fig. 10. It can be seen that the diffusion coefficients in both alloys without fibers can be well described by Arrhenius equation $D = D_0 \exp(-Q/RT)$ – see the straight lines in Fig. 10. Respective values of pre-exponential factor D_0 and activation enthalpy Q are listed in Table 3.

3.4. Temperature dependence of D_{eff} and D_i

In contrast to D_v, diffusion coefficients D_{eff} and D_i show a non-Arrhenius behavior in the temperature interval 648 – 728 K. It is obvious in Fig. 10 that there is a tendency to enhanced value of D_{eff} (and therefore also D_i) in the middle of the temperature interval, which is emphasized graphically by the broken dashed lines (they guide the eye only). The explanation we propose is based on the temperature dependence of local strains close to the matrix/fiber interfaces. In [5], thermal expansion behavior was studied of short fiber reinforced Mg composites. It was observed that above a certain inverse temperature T_i, the CTE starts to decrease with increasing temperature and it goes

through a local minimum. The process can be rationalized as follows: Within the metal-matrix composites reinforced by ceramic fibers, there is always an internal stress caused by considerable difference in CTE's of both components. At inverse temperature T_i, the elastic accommodation ability of the matrix close by fibers is exhausted and the release of the thermally induced stress must be realized by inhomogeneous plastic deformation of the matrix before all in the vicinity of the interphase boundary. This is accompanied by a local increase of dislocation density. The minimum of CTE of the composite reflects, most likely, the strengthening of the area, i.e., the state with a maximum dislocation density. The diffusion measurements reported in the present paper were carried out exclusively at temperatures above T_i , where the plastic mode of the stress relaxation prevails the elastic one. It can be seen in Fig. 10 that the break point on the measured temperature dependences of D_{eff} (and D_i) are close to the temperature $T_{min\ CTE}$ where the minimum in CTE was detected in [5] in the first run of the cycling thermal expansion test. Hence, the up-ward curvature of observed temperature dependences of D_{eff} and D_i may be due to enhanced dislocation density at temperatures close to 693 K.

3.5. Comparison of AZ91(S) and QE22(S)

It can be seen in Fig. 10 that ^{65}Zn diffusion coefficients in QE22(S) are systematically lower than respective values for diffusion in AZ91(S). This relation may be put in instructive relation to some other physical properties and empiric limitations – see in Table 4. It is obvious that the observed relation of diffusion coefficients agrees qualitatively with the empiric rule that relates the diffusion rates in different materials to their solidus T_s (or melting) temperature [16]. Ratio of observed diffusion characteristics in reinforced alloys agrees also with the ratios of creep and strength characteristics – the

alloy QE22S shows higher resistance against mechanical loading. The onset of plastic deformation of this material (measured by T_i) occurs at higher temperatures. These facts – among others – led to a higher value of recommended service temperature T_{max} of QE22S for engineering applications [1].

It can be summarized that the higher diffusion coefficient of Zn in AZ91 compared to that in QE22 is coupled with higher strength of the QE22 lattice. In case of strengthened alloys AZ91S and QE22S, lower effective (and interfacial) diffusivity in QE22S may be due to lower dislocation density in the deformed matrix close to the fiber/matrix interfaces.

Summary

Diffusion coefficient, D_v, of zinc in matrix alloys AZ91 and QE22, effective diffusion coefficient of zinc, $D_{eff,}$ in two-phase Saffil-reinforced composites AZ91S and QE22S, and interface diffusion coefficient of zinc, D_i, in the interface between the Saffil fibers and matrix was measured by serial sectioning method in the temperature interval 648 – 728 K. Since zinc is one of component of the AZ91(S) alloy and his diffusion behavior can be taken for similar to that of Ag, which is a component of QE22(S) alloy [17], the measured values of diffusion coefficients can be used for quantitative estimation of rate of diffusion-controlled processes running in studied alloys both during the production and during the service of the final product. Ratio of diffusion coefficients measured in the two types of alloys reflects qualitatively the ratio of chosen strength characteristics of the both alloys.

Acknowledgments

The work was supported by the Czech Science Foundation (project number 106/05/2115) and by the Academy of Sciences of the Czech Republic (project number AV0Z20410507).

References

[1] Avedesian M, Baker H. Magnesium and magnesium alloys. ASM Materials Park; 1999.

[2] Lukáč P, Rudajevová A. Thermal expansion in magnesium composites. Kovove Mater 2003;41:281–292.

[3] Rudajevová A, Balík J, Lukáč P. Thermal expansion behaviour of Mg-Saffil fibre composites. Mater Sci Eng A 2004;387–389:892–895.

[4] Kumar S, Mondal AK, Dieringa H, Kainer KU. Analysing hysteresis and residual strains in thermal cycling curves of short fibre reinforced Mg-MMCs. Compos Sci Technol 2004;64:1179–1189.

[5] Rudajevová A, Padalka O. Thermal expansion of pre-deformed, short fibre reinforced Mg-based composites. Compos Sci Technol 2005;65:989–995.

[6] Rudajevová A, Musil O. Influence of the interface on the thermal expansion and thermal conductivity of QE22 based composites. Kovove Mater 2005;43:210–217.

[7] Rehman FU, Fox S, Flower HM, West DRF. Fibre/matrix interactions in magnesium-based composites containing alumina fibres. J Mater Sci 1994;29:1636–1644.

[8] Massalski TB. Binary alloy phase diagrams. ASM International, ASM/NIST, CD-ROM; 1996.

[9] Hutchinson CR, Nie JF, Gorsse S. Modeling the precipitation processes and strengthening mechanisms in a Mg-Al-(Zn) AZ91 alloy. Metall Mater Trans A 2005;36:2093–2105.

[10] Kiehn J, Smola B, Vostrý P, Stulíková I, Kainer KU. Microstructure changes in isochronally annealed alumina fibre reinforced Mg-Ag-Nd-Zr alloy. Phys Stat Sol (a) 1997;164:709–723.

[11] Rakowska A, Socjuzs-Podosek M, Litynska L, Ciach R. Analytical electron microscopy of a magnesium alloy containing neodymium. Microchimica Acta 2002;139:145–149.

[12] Kaur I, Mishin Y, Gust W. Fundamentals of grain and interphase boundary diffusion. Chichester, New York, Brisbane, Toronto, Singapore: J. Wiley & Sons LTD; 1995.

[13] Crank J. Mathematics of diffusion. Oxford: Clarendon Press; 1957.

[14] Le Gall M, Lesage B. Self-diffusion in α-Al_2O_3 I. Aluminium diffusion in single crystals. Philos Mag A 1997;70:761–773.

[15] Belova IV, Murch, GE. The effective diffusivity in polycrystalline material in the presence of interphase boundaries. Philos Mag 2004;84:17–28.

[16] Shewmon P. Diffusion in solids. Warrendale, Pennsylvania: TMS; 1989.

[17] Nonaka K, Sakazawa, T, Nakajima H. Reaction diffusion in Mg-Cu system. Mater Trans JIM 1995;36:1463–1466.

[18] Sklenička V, Pahutová M, Kuchařová K, Svoboda M, Langdon TG. Creep processes in magnesium alloys and their composites. Metall Mater Trans A 2002;33:883–889.

Table 1

Diffusion coefficients D_v in AZ91, effective diffusion coefficients D_{eff} and diffusion coefficients D_i in interfaces between the matrix and fibers in AZ91S. L – mean diffusion path in the bulk.

T (K)	t (s)	D_v ($m^2 s^{-1}$)	$L = 2\sqrt{D_v t}$ (μm)	D_{eff} ($m^2 s^{-1}$)	D_i ($m^2 s^{-1}$)
728	7200	2.75×10^{-13}	86	2.42×10^{-12}	2.90×10^{-8}
708	18000	1.23×10^{-13}	94	9.15×10^{-13}	1.10×10^{-8}
688	25200	9.79×10^{-14}	99	1.47×10^{-12}	1.67×10^{-8}
668	54000	4.66×10^{-14}	100	2.67×10^{-13}	3.20×10^{-9}
648	72000	1.81×10^{-14}	72	1.15×10^{-13}	1.38×10^{-9}

Table 2

Diffusion coefficients D_v in QE22, effective diffusion coefficients D_{eff} and diffusion coefficients D_i in interfaces between the matrix and fibers in QE22S. L – mean diffusion path in the bulk.

T (K)	t (s)	D_v ($m^2 s^{-1}$)	$L = 2\sqrt{D_v t}$ (μm)	D_{eff} ($m^2 s^{-1}$)	D_i ($m^2 s^{-1}$)
728	7200	1.08×10^{-13}	28	2.19×10^{-13}	1.51×10^{-9}
708	18000	5.25×10^{-14}	31	1.85×10^{-13}	1.28×10^{-9}
688	25200	2.68×10^{-14}	26	1.70×10^{-13}	1.17×10^{-9}
668	54000	1.28×10^{-14}	26	8.75×10^{-14}	6.03×10^{-10}
648	72000	8.83×10^{-15}	25	3.13×10^{-14}	2.16×10^{-10}

Table 3

Arrhenius parameters for ^{65}Zn diffusion in AZ91 and QE22.

	$-\ln D_0$ D_0 in $m^2\ s^{-1}$	Q (kJ mol^{-1})
D_v in AZ91	8.1 ± 2.1	128 ± 12
D_v in QE22	9.3 ± 1.7	125 ± 10

Table 4

Relation of chosen characteristics of AZ91(S) (upper index 1) and QE22(S) (upper index 2). σ_Y – yield strength (MPa), $\dot{\varepsilon}_m$ - minimum creep rate (s^{-1}), T_s – solidus (K), T_i – inverse temperature of CTE (K), T_{max} - maximum recommended service temperature (K), S – reinforced by Saffil fibers.

Property ratio	remarks		Numeric ratio		Ref.
σ_Y^1 / σ_Y^2	tensile; 283 K		145 / 195	< 1	[1]
$\dot{\varepsilon}_m^1 / \dot{\varepsilon}_m^2$	at σ = 90 MPa	S	$10^{-8} / 10^{-10}$	> 1	[18]
T_s^1 / T_s^2			741 / 808	< 1	[1]
T_i^1 / T_i^2		S	493 / 573	< 1	[2, 5]
D_v^1 / D_v^2	648 – 728 K		~ 3.3	> 1	this work
$D_{eff}^1 / D_{eff}^2 \left(= D_i^1 / D_i^2\right)$	648 – 728 K	S	~ 9	> 1	this work
T_{max}^1 / T_{max}^2			403 /523	< 1	[1]

Figure captions

Fig. 1 Optical micrograph of AZ91 after 693 K / 15 h (+ 728 K / 2 h). Light sheets at grain bundaries – $Mg_{17}Al_{12}$. Polarized light; etched in C_2H_5OH (100 ml), H_2O (18 ml), CH_3COOH (6 ml), picric acid (12 g).

Fig. 2 SEM micrograph of AZ91S after 693 K / 15 h (+ 728 K / 2 h). Polished with OP-S suspension; back-scattered-electron regime (BSE). Light particles – $Mg_{17}Al_{12}$.

Fig. 3 SEM micrograph of QE22 after 798 K / 8 h (+ 728 K / 2 h). Polished with diamond paste; secondary-electron regime (SE). Light particles – Nd-rich precipitates – see the text.

Fig. 4 SEM micrograph of QE22S after 798 K / 8 h (+ 728 K / 2 h). Polished with OP-S suspension; SE regime.

Fig. 5 SEM micrograph of QE22S after 798 K / 8 h (+ 728 K / 2 h). Polished with OP-S suspension; SE regime. Light particles – Nd-rich precipitates.

Fig. 6 Penetration profiles $c(x,t)$ of ^{65}Zn in AZ91.

Fig. 7 Penetration profiles $c(x,t)$ of ^{65}Zn in QE22.

Fig. 8 Penetration profiles $c(x,t)$ of ^{65}Zn in AZ91S.

Fig. 9 Penetration profiles $c(x,t)$ of ^{65}Zn in QE22S.

Fig. 10 Arrhenius diagram of measured diffusion coefficients: D_v – volume diffusion in matrix alloys, D_{eff} – effective diffusion in two-phase fiber reinforced composites, D_i – diffusion in interfacial regions (in matrix close to the matrix/fiber interface). Full lines – fitted Arrhenius equation $D = D_0 \exp(-Q / RT)$, dashed lines – for guide the eye only, $T_{min\ CTE} \cong 693$ K – temperature, where the CTE in Mg composite is minimal [5].

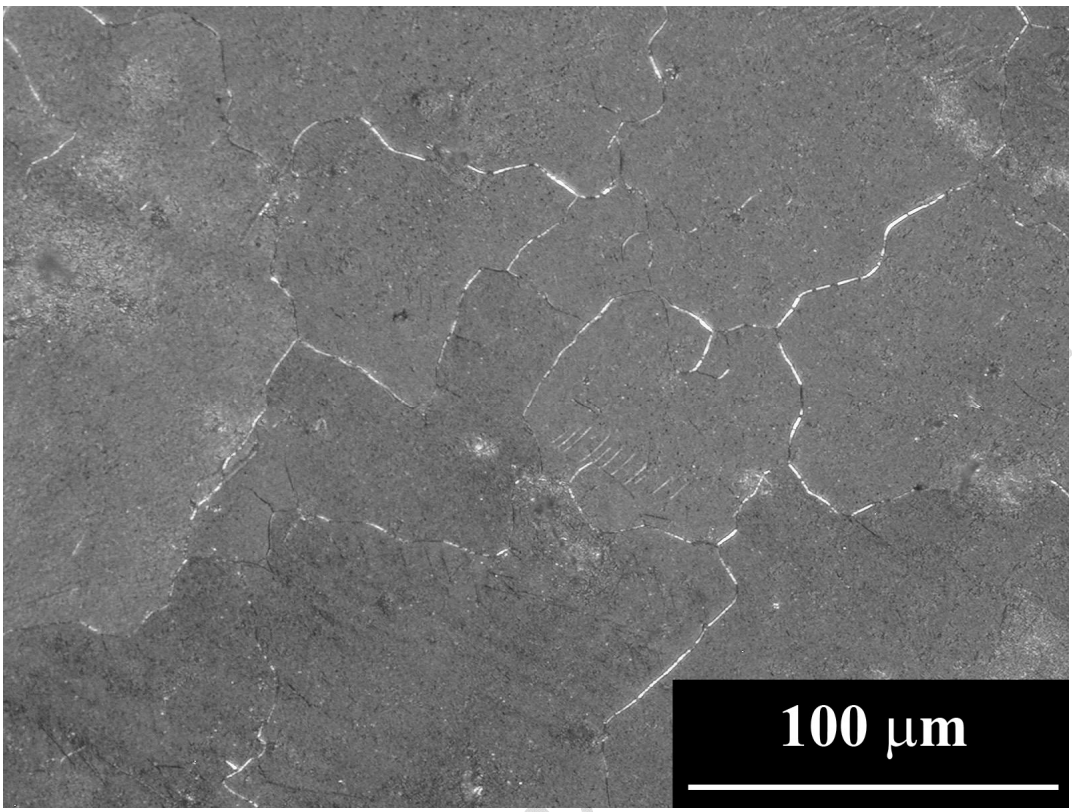

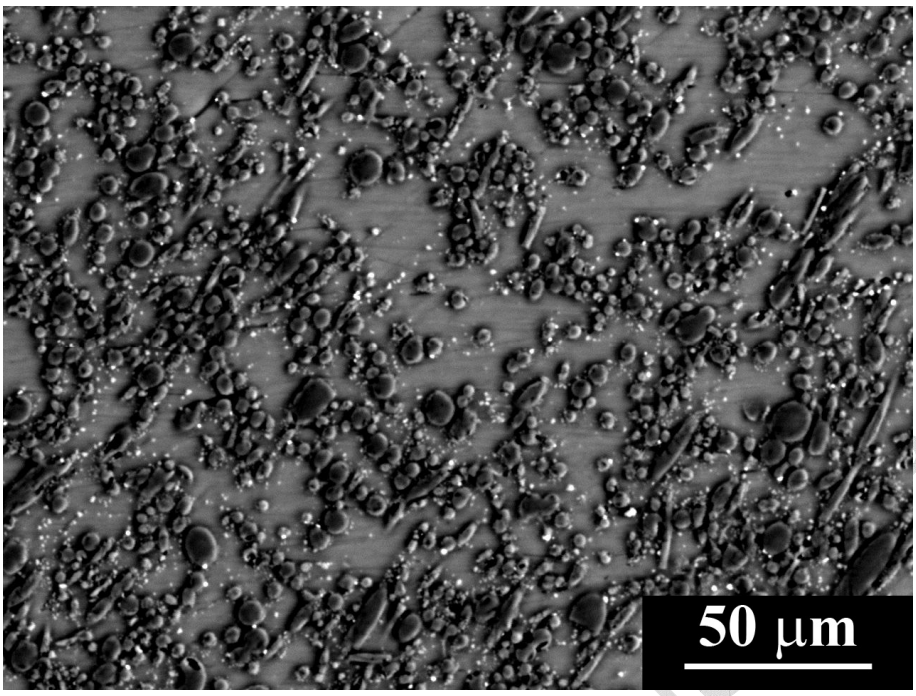

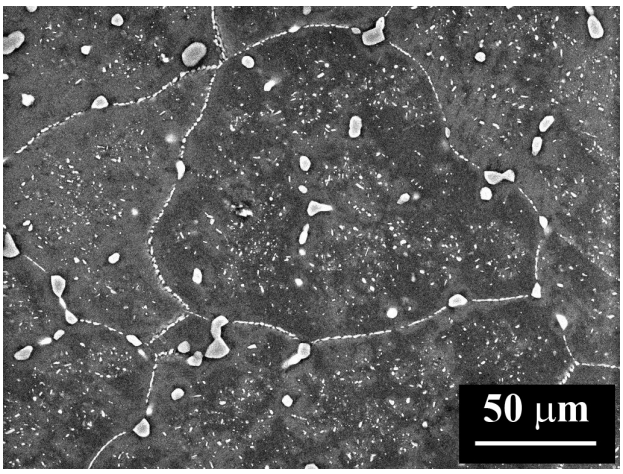

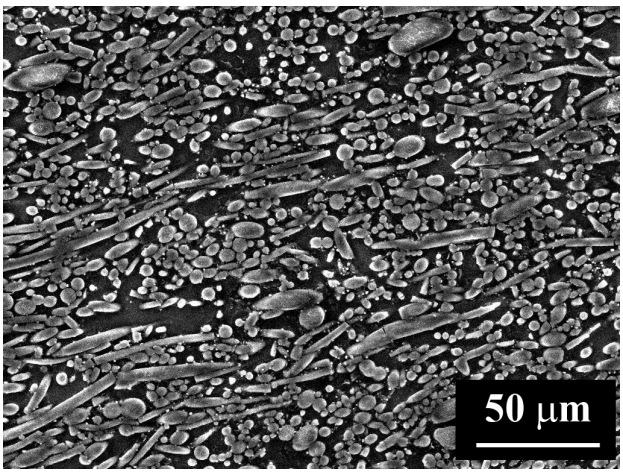

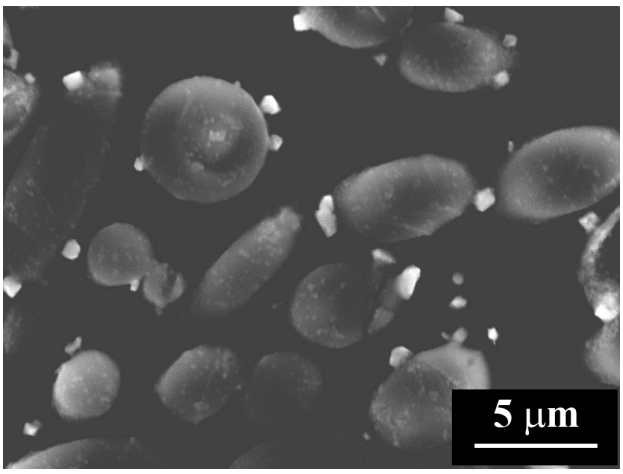

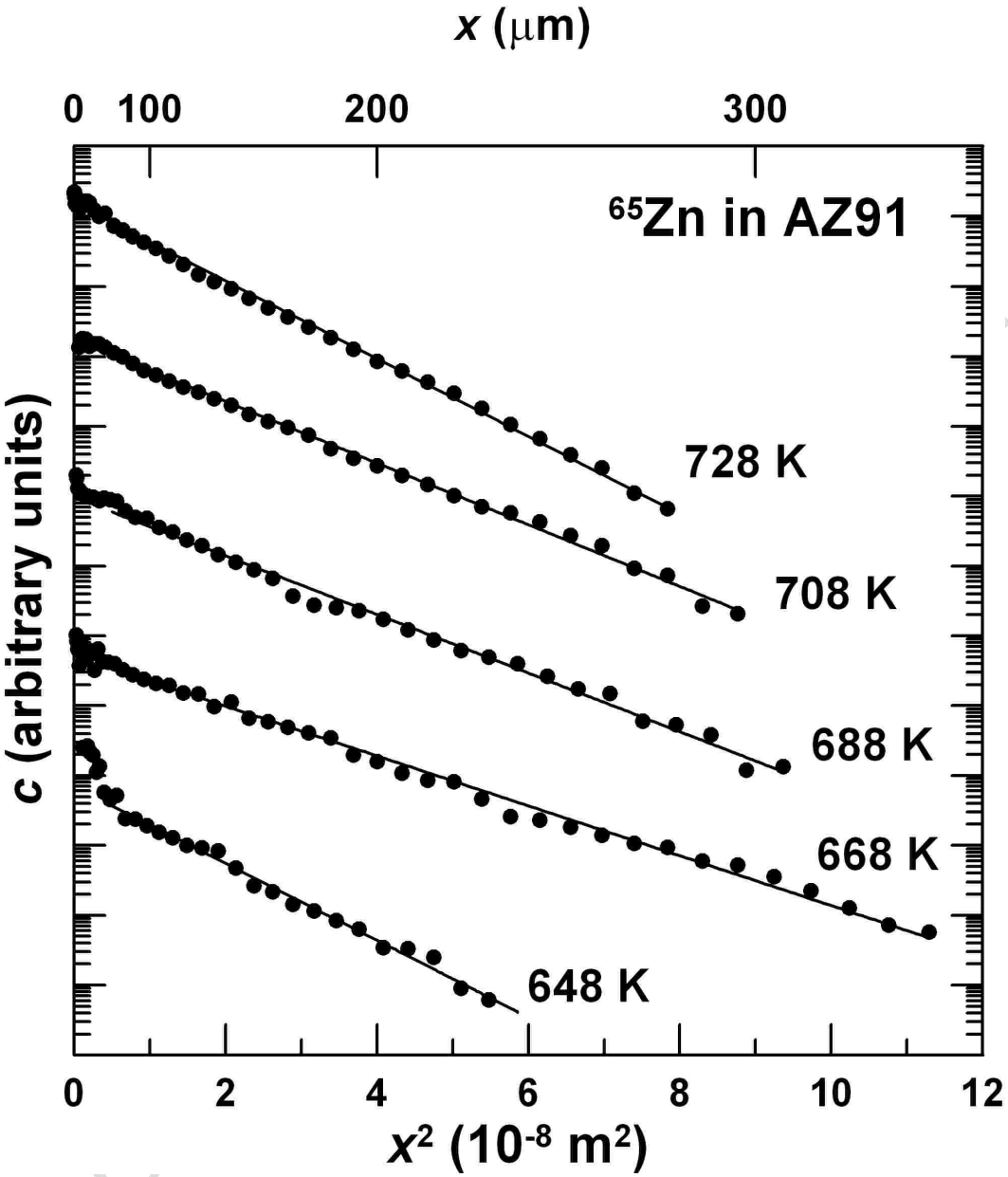
x (μm)
0
100
200
300
65Zn in AZ91
728 K
708 K
688 K
668 K
648 K
c (arbitrary units)
0
2
4
6
8
10
12
x2 (10-8 m2)

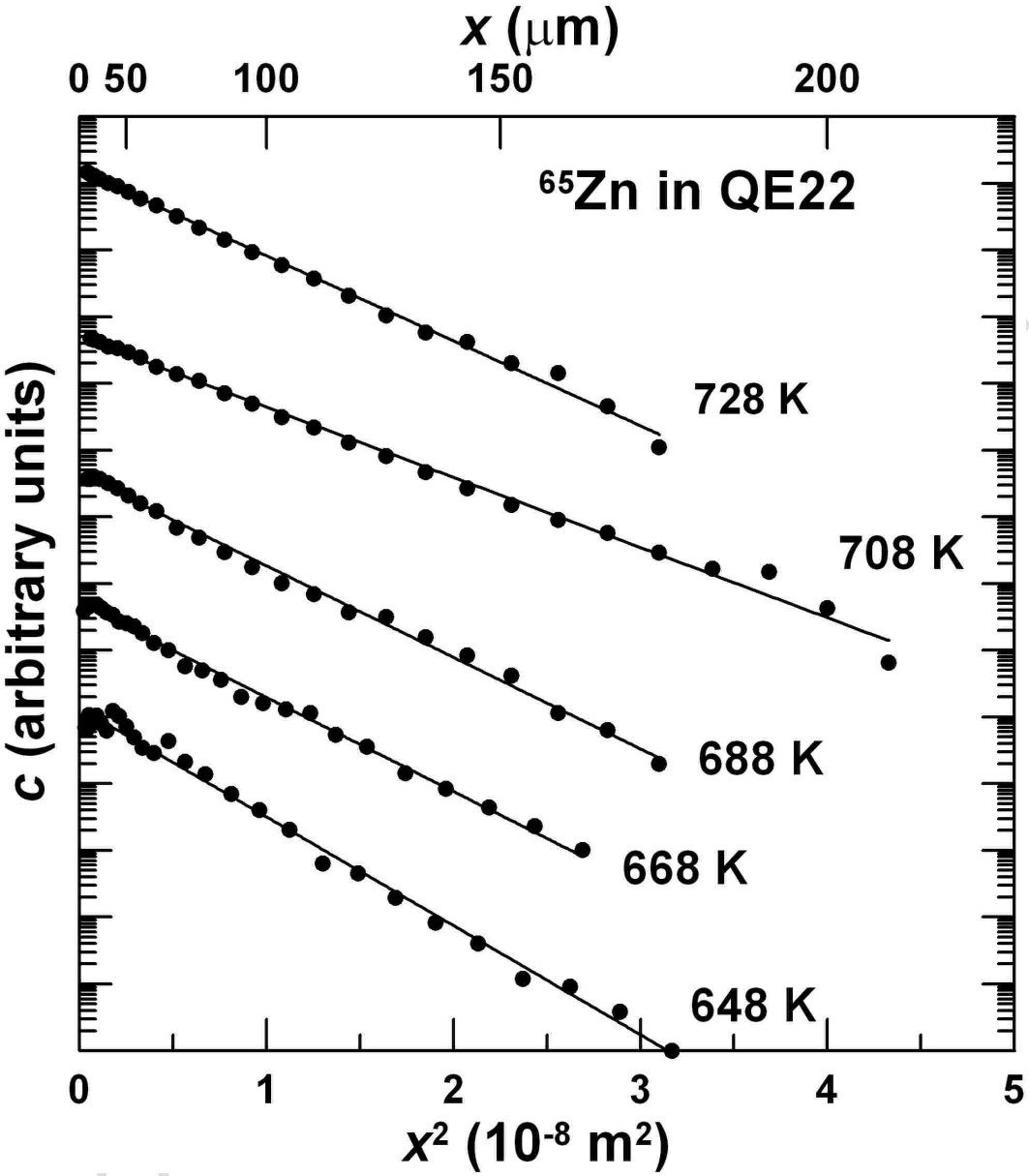
x (μm)
0 50
100
150
200
65Zn in QE22
728 K
708 K
688 K
668 K
648 K
c (arbitrary units)
0
1
2
3
4
5
x2 (10-8 m2)

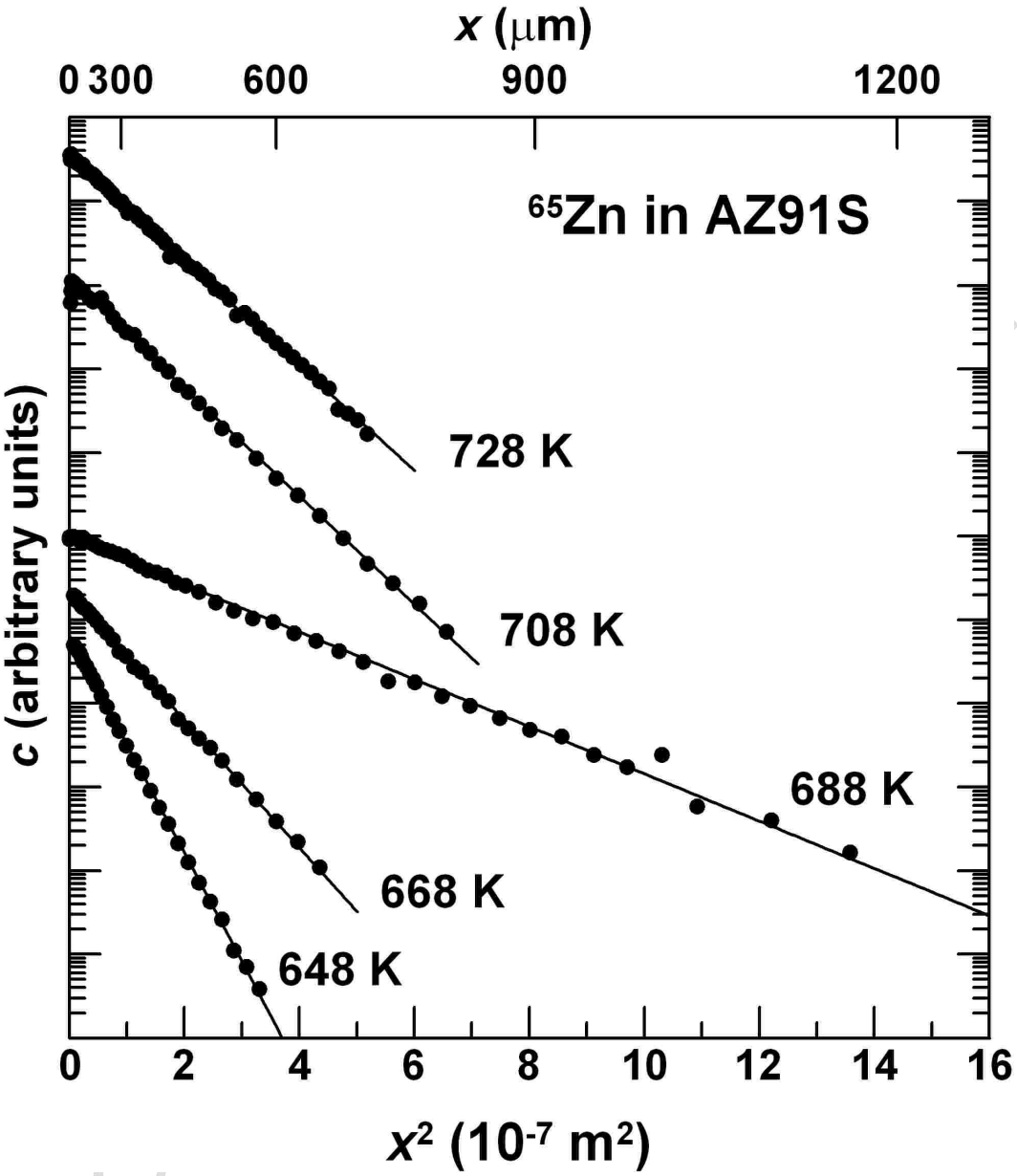
x (μm)
0 300
600
900
1200
65Zn in AZ91S
728 K
708 K
688 K
668 K
648 K
c (arbitrary units)
0
2
4
6
8
10
12
14
16
x2 (10-7 m2)

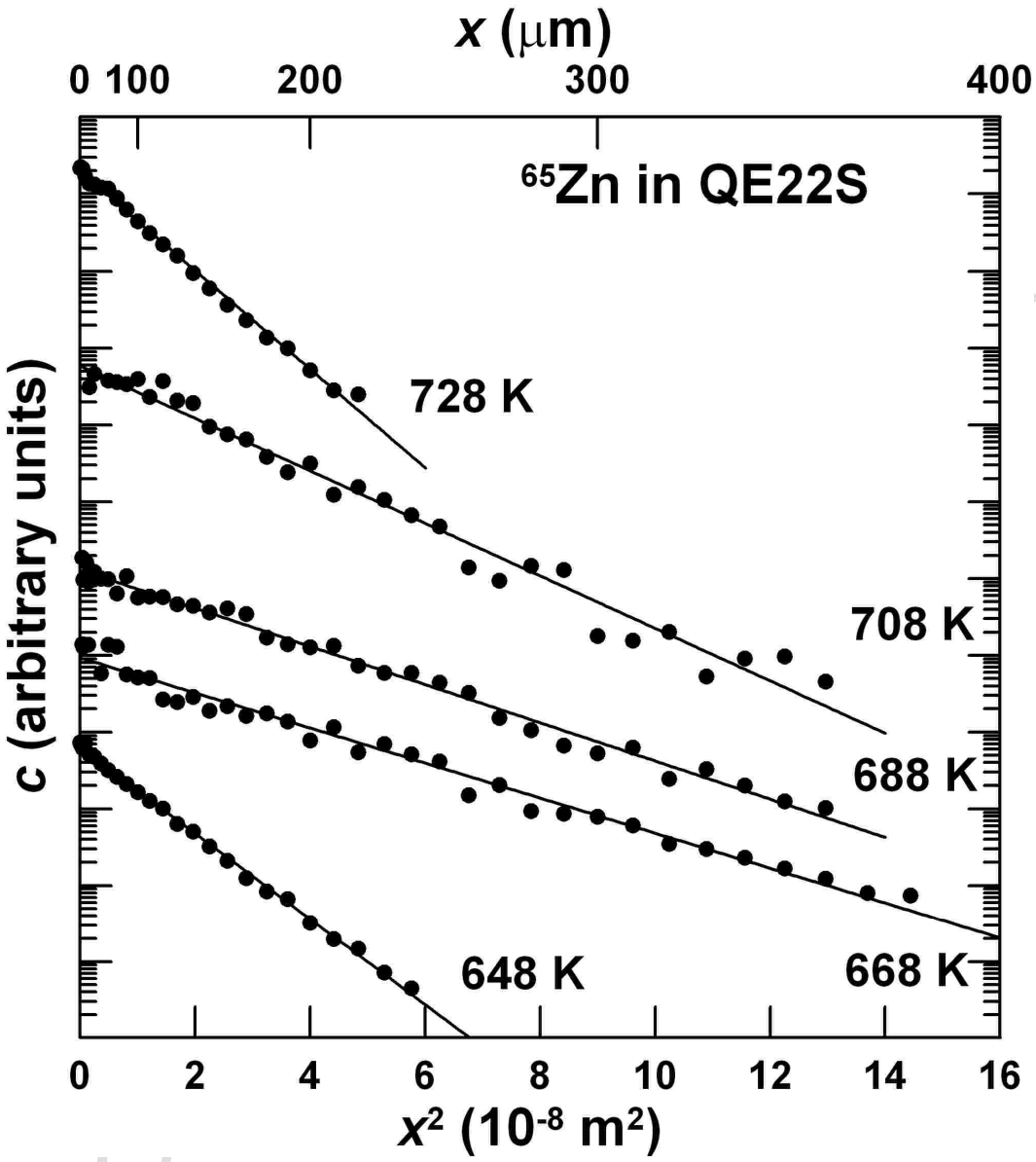
x (μm)
0 100
200
300
400
65Zn in QE22S
728 K
708 K
688 K
668 K
648 K
c (arbitrary units)
0
2
4
6
8
10
12
14
16
x2 (10-8 m2)

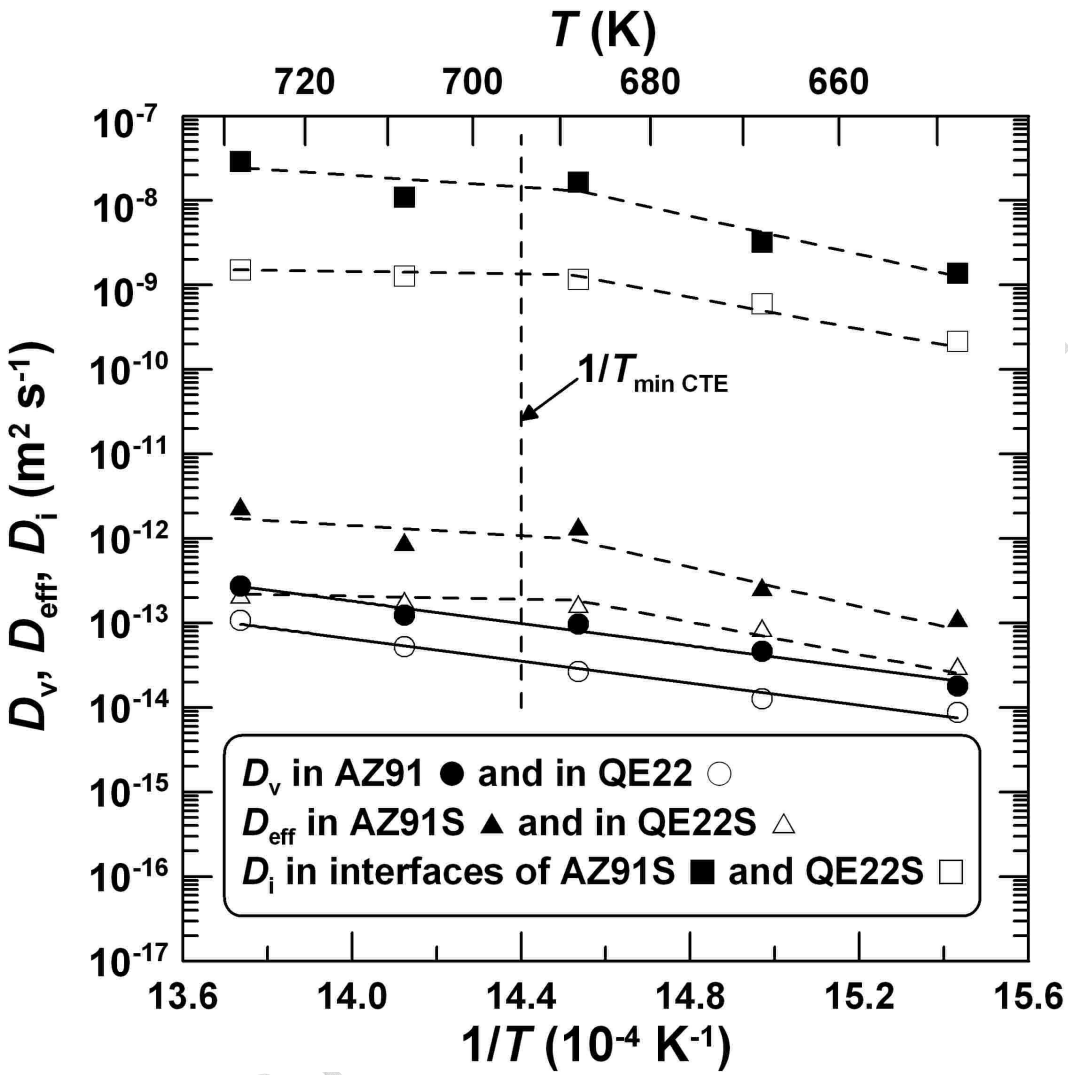
T (K)
720
700
680
660
10-7
10-8
10-9
10-10
10-11
10-12
10-13
10-14
10-15
10-16
10-17
Dv, Deff, Di (m2 s-1)
1/Tmin CTE
Dv in AZ91 ● and in QE22 ○
Deff in AZ91S ▲ and in QE22S △
Di in interfaces of AZ91S ■ and QE22S □
13.6
14.0
14.4
14.8
15.2
15.6
1/T (10-4 K-1)